ESTIMATING THE PLANT NITROGEN CONTENT OF FOXTAIL MILLET (*SETARIA ITALICA* L.) BASED ON CONTINUOUS WAVELET ANALYSIS

XIA, F.[1,2] – FENG, M. C.[1,2*] – ZHU, S. A.[1,2] – WANG, C.[1,2] – MU, T. T.[1,2] – XIAO, L. J.[1] – YANG, W. D.[1,2] – ZHANG, M. J.[1] – SONG, X. Y.[1,2] – YANG, H.[3] – QIN, M. X.[4]

[1]*Agronomy College, Shanxi Agricultural University, Taigu 030800, Shanxi, China*

[2]*State Key Laboratory of Sustainable Dryland Agriculture (in preparation), Shanxi Agricultural University, Taiyuan 030000, Shanxi, China*

[3]*College of Information Science and Engineering, Shanxi Agricultural University, Taigu 030800, Shanxi, China*

[4]*College of Resource and Environment, Shanxi Agricultural University, Taigu 030800, Shanxi, China*

**Corresponding author*
e-mail: fmc101@163.com; phone: +86-138-3483-8834

(Received 21st Apr 2022; accepted 22nd Jul 2022)

Abstract. The variation in the plant nitrogen content (PNC) directly characterizes the growth of foxtail millet, and estimation of the PNC using hyperspectral techniques is important for effective evaluating the growth of this species. Effective statistical modeling methods can improve the accuracy and reliability of PNC estimates. In this study, field experiments were conducted under different gradients of organic fertilizer to develop an estimation model for determining the PNC in foxtail millet. The continuous wavelet transform (CWT) was used to process the collected reflection spectra and construct partial least square regression (PLSR), random forest (RF) and support vector machine (SVM) estimation models. Among the common wavelet families, Daubechies (db5), Coiflets (coif3), Biorthogonal (bior1.5), Symlets (sym8), haar and rbio3.1 were selected to analyze the correlation with the PNC, and all the wavelet functions had a good correlation with the PNC. The correlation coefficients were 0.834, -0.835, -0.973, -0.784, -0.789 and -0.770, respectively. The CWT technique can significantly improve the prediction accuracy of the PNC. The best PNC estimate was obtained using db5 (R^2_{cal} = 0.859, $RMSE_{cal}$ = 3.415), and the best decomposition scale was 2^4. In addition, the validation data indicate that db5-RF can be used to estimate the PNC (R^2_{val} = 0.935, $RMSE_{val}$ = 1.311, RPD_{val} = 3.32). This study provides a reference for the practical application of PNC analysis in foxtail millet.
Keywords: *hyperspectral data analysis, wavelet transform, partial least square regression, support vector machine, random forest*

Abbreviations: R^2_{cal}, coefficient of determination of the calibration set; $RMSE_{cal}$, root mean square error of the calibration set; R^2_{val}, coefficient of determination of the validation set; $RMSE_{val}$, root mean square error of the validation set; RPD_{val}: residual prediction deviation of the validation set

Introduction

Foxtail millet (*Setaria italica* L.) is a healthy staple food originating in China and is listed as the most common small grain among Chinese crops (Lu et al., 2009). Foxtail millet has a short planting cycle, a high drought tolerance, and a strong ability to adapt to adverse climate conditions; it is widely cultivated in arid and semiarid regions of the world, especially in China and India (Mahajan et al., 2021; Jia et al., 2013). Nitrogen, an essential nutrient for crops, has an important influence on crop photosynthesis and

http://www.aloki.hu ● ISSN 1589 1623 (Print) ● ISSN 1785 0037 (Online)
DOI: http://dx.doi.org/10.15666/aeer/2005_43914407

quality. Therefore, real-time adjustment of the nitrogen supply is an important task to ensure that cereal crops grow well and produce high quality and stable yields, while an effective, non-destructive, and low-cost method or tool for measuring the nitrogen content in the field is also a key step in accurate fertilization (Bechlin et al., 2014; Eitel et al., 2014; Mao et al., 2015).

In recent years, many methods have been used to determine the crop nitrogen status. The traditional method of determining the nitrogen status involves collecting samples from the field and analyzing them based on chemical methods. However, this method is characterized by hysteresis, destructiveness, and high costs (Dong et al., 2010; Tian et al., 2014). Compared with traditional sampling methods, remote sensing methods provide fast, non-destructive, and dynamic monitoring approaches for estimating the physiological parameters and nutrient levels of crops; these methods have attracted a substantial amount of attention in crop nitrogen monitoring (He et al., 2016; Clevers et al., 2017; Hong et al., 2018; Li et al., 2016).

A vegetation index has been used to successfully monitor the nitrogen content of winter wheat leaves (Feng et al., 2016). Tarpley et al. (2000) reported that the red edge position and the near-infrared band can be combined to accurately estimate the nitrogen content in cotton leaves. Ranjan et al. (2012) used hyperspectral remote sensing to build an estimation model of the nitrogen content of wheat leaves and aboveground nitrogen accumulation. The results showed that the estimation accuracy of the vegetation index for the leaf nitrogen content was better than that for aboveground nitrogen accumulation. Li et al. (2018c) analyzed the nutritional status of the leaf nitrogen content and plant nitrogen accumulation in winter wheat in different years and growth stages based on the N-PROSAIL model, and the results showed that this method can effectively estimate the nitrogen status of winter wheat. Stroppiana et al. (2009) estimated the nitrogen content of rice based on hyperspectral data and found that nitrogen regression constructed by using spectral reflectance information from the blue and green light bands can accurately reflect the nitrogen nutritional status of rice. However, the influence of the nitrogen content on crop spectra is hidden in the spectral signal, and the use of band screening or spectral indices (Datt, 1999) in spectral analysis methods leads to the loss of some hidden information in the hyperspectral data, resulting in a relatively low estimation accuracy.

The continuous wavelet transform (CWT) is an effective signal processing method (Blackburn et al., 2008); it uses a wavelet function to decompose spectral reflectance at different scales into a series of wavelet energy coefficients, and correlation analysis is then conducted with the physiological and biochemical parameters of crops (Tao et al., 2012). The wavelet coefficients obtained from spectral data and processing are not sensitive to background interference and the external environment and are highly correlated with physiological parameters. At the same time, the regression model between wavelet coefficients and physiological parameters can be established to improve the precision of the inversion model (Rivard et al., 2008). Ampe et al. (2013) established an estimation model of the chlorophyll content in inland water bodies based on continuous wavelet analysis, and the prediction accuracy of the model exceeded that of the traditional blue–green band ratio method. Wang et al. (2016) reported that SPAD can be estimated using the CWT method with a high coefficient of determination (coefficient of determination (R^2) = 0.7444, root mean square error (RMSE) = 7.359). Cheng et al. (2010) used the CWT to analyze a dataset of 47 plant species and compared it with the vegetation index analysis method. The estimation accuracy of the wavelet

http://www.aloki.hu ● ISSN 1589 1623 (Print) ● ISSN 1785 0037 (Online)
DOI: http://dx.doi.org/10.15666/aeer/2005_43914407

transform approach was much higher than that of the vegetation index-based method. Zhang et al. (2014) used the traditional wheat spectrum and the continuous wavelet characteristic spectrum to determine the physiological condition of wheat. The results showed that the physiological response of the wavelet characteristic spectrum to wheat was stronger than that of the original spectrum, and the proposed approach performed well in estimating the physiological potential. Continuous wavelet analysis adds a new dimension to the establishment of plant physiological parameter estimation models using spectral data (Cheng et al., 2014).

Hyperspectral remote sensing systems with different spectral, spatial, and temporal characteristics provide a large amount of hyperspectral data for the monitoring of nitrogen in cereal crops. However, hyperspectral data usually contain highly correlated bands, and cereal crop nitrogen monitoring models fitted directly with such data are prone to overfitting, which limits the accuracy of such models (Rivera-Caicedo et al., 2017; Thorp et al., 2017). In recent years, machine learning algorithms with higher accuracies have been used to solve the variable covariance problem to a large extent and deal with high-dimensional data (Marang et al., 2021). The effectiveness of machine learning algorithms has been proven in the field of hyperspectral research, and the advantages of theses algorithms, which include the support vector machine (SVM) (Chen et al., 2022) and random forest (RF) (Chen et al., 2020) algorithms, over multiple linear regression in describing the complex relationship between the crop nitrogen status and hyperspectral data are becoming increasingly clear (Tan et al., 2017; Zhou et al., 2018). Thus, this study aimed to clarify and create a monitoring method to estimate the plant nitrogen content PNC of foxtail millet on the basis of the CWT and the partial least square regression (PLSR), SVM and RF algorithms during the growth stages. An appropriate wavelet function was chosen to perform scale 2^1-2^{10} decomposition of the spectral reflectance to obtain the wavelet coefficients and perform correlation analysis. The PLSR, RF and SVM estimation models were constructed based on the optimal decomposition scales obtained from the CWT and the correlation analysis. The accuracy of the four models under different wavelet functions was explored, and the best wavelet function and model were determined to provide a foundation for the practical application of nitrogen content analysis in foxtail millet.

Materials and methods

Experimental design

The experiment was conducted in Shanyin County, Shuozhou city, Shanxi Province (39°11’-39°47’ N, 112°25’-113°04’ E) from May to October 2019. The local climate in this area is a temperate continental monsoon climate with an average annual temperature of approximately 7 °C and an average annual rainfall of 410 mm. The experiment adopted a split zone design, with the main zone including Jingu21 and Jingu28. The subsidiary zone was treated with sheep dung as an organic fertilizer (the recommended amount was 7881.8 $kg \cdot hm^{-2}$, organic matter $\geq 50\%$ and nitrogen, phosphorus and potassium $\geq 5\%$). The organic fertilizer applications were set as follows: T0: compound fertilizer control treatment (the recommended amount was 750 $kg \cdot hm^{-2}$; the ratio of nitrogen to phosphorus to potassium was 24:10:6), T1: 5763.6 $kg \cdot hm^{-2}$, T2: 7881.8 $kg \cdot hm^{-2}$, T3: 10000 $kg \cdot hm^{-2}$ and T4: 0 $kg \cdot hm^{-2}$. Each treatment was repeated three times.

http://www.aloki.hu ● ISSN 1589 1623 (Print) ● ISSN 1785 0037 (Online)
DOI: http://dx.doi.org/10.15666/aeer/2005_43914407

Foxtail millet canopy spectrum

The canopy spectra of foxtail millet at the four growth stages BBCH 32, 47, 55, and 70 (Bleiholder et al., 2001) were recorded. BBCH stands for Biologische Bundesanstalt, Bundessortenamt and Chemical industry. The BBCH-scale is based on the well-known cereal code developed by Zadoks et al. (1974). The canopy spectra of plants were determined using a portable FieldSpec Pro hyperspectral radiometer (FR2500, American Analytical Spectral Device, ASD). An ASD non-imaging spectrometer with a band range of 350-2500 nm and a field of view of 25° was used. The sampling interval from 350-1000 nm was 1.4 nm, and the spectral resolution was 3 nm. The sampling interval of the 1000-2500 nm spectrum was 2 nm, and the spectral resolution was 10 nm. To eliminate the influence of environmental conditions spectra were collected in clear and windless weather between 10:00 and 14:00 local time. The instrument was adjusted by white standard calibration each quarter, and the probe was oriented vertically downward at a vertical height of approximately 1 m from the canopy. Three representative sampling points were selected within the plot, ten readings were obtained for each point (n = 30), and the average value was used as the final spectrum of each plot.

PNC determination

The PNC was measured simultaneously with spectral measurements based on canopy spectroscopy. A total of 120 plant samples were used for PNC determination. The selected plants were desiccated at 105 °C for 30 min and then dried at 80 °C to constant weight. The sample was crushed and sieved, 0.5 g of powder was weighed, 5 mL of concentrated H_2SO_4 was added, and the resulting mixture was placed in a digestion oven at 370 °C. Hydrogen peroxide was used as a catalyst. The nitrogen concentration was measured with a Smart-chem 200 automatic chemical analyzer produced by Alliance in France.

CWT

Wavelet analysis can be used to decompose complex spectral signals into wavelet signals of different scales (frequencies). This method can be used to perform multiscale decomposition and mainly involves the extraction of information as a function of time and space frequencies. Wavelet transform types can be divided into the CWT and the discrete wavelet transform (DWT). When the DWT is used to analyze hyperspectral data, determining the output parameters is difficult. Therefore, this study used the CWT to transform the foxtail millet spectrum curves. The wavelet function scales and shifts can be obtained from the following equation (Lin et al., 2021):

$$\Psi_{a,b}(t) = \frac{1}{\sqrt{a}} \Psi\left(\frac{t-b}{a}\right) \quad \text{(Eq.1)}$$

where $\Psi_{a,b}(t)$ is the wavelet function; a is a scale factor; and b is a translation factor. The output of the CWT is given by the following:

$$Wf(a,b) \leq f; \Psi_{a,b} \geq \int_{-\infty}^{+\infty} f(t)\, \Psi_{a,b}(t) dt \quad \text{(Eq.2)}$$

http://www.aloki.hu ● ISSN 1589 1623 (Print) ● ISSN 1785 0037 (Online)
DOI: http://dx.doi.org/10.15666/aeer/2005_43914407

where $Wf(a_i, b_j)$ are the CWT coefficients of a two-dimensional wavelet power scalogram (j = 1, 2, …, n) that is composed of a noe-dimensional scale (i = 1, 2, …, m). *f(t)* is the hyperspectral reflectance data; and t is the spectral band. The wavelet function of the wavelet transform is not unique, the results of different wavelet functions are not the same, and the wavelet function is selected based on the support length, symmetry, vanishing moment, regularity and similarity. In this study, six common wavelet families (Daubechies (db5), Coiflets (coif3), Biorthogonal (bior1.5), Symlet (sym8), haar and rbio3.1) were selected to process the hyperspectral data (Virmani et al., 2013). The original reflectance spectrum data from the samples were decomposed with a 10-layer wavelet in MATLAB, and the decomposition scale of the CWT was set to 2^1, 2^2, 2^3..., and 2^{10}.

Model construction and verification

To evaluate the estimation accuracy and stability of the model, the R^2, RMSE, residual prediction deviation (RPD) and 1:1 line were used (Viscarra et al., 2007). The R^2 and RPD evaluation criteria are shown in *Table 1*. A 1:1 scatter plot was created to visually demonstrate the reliability of the PNC model. The formulas for R^2, RMSE and RPD are as follows (Wang et al., 2020a):

$$R^2 = 1 - \frac{\sum_{i=1}^{n}(y_i - x_i)^2}{\sum_{i=1}^{n}(y_i - \bar{y})^2} \quad \text{(Eq.3)}$$

$$RMSE = \sqrt{\frac{\sum_{i=1}^{n}(x_i - y_i)^2}{n}} \quad \text{(Eq.4)}$$

$$RPD = \frac{SD}{RMSE} \quad \text{(Eq.5)}$$

where n is the number of samples, x_i and y_i are the predicted value and the measured value respectively, $\bar{y}$ is the average of the measured value, and SD is the standard deviation.

Table 1. *Classification of the accuracy of the model based on the R^2 and RPD values*

Parameters	Model accuracy		
	Unacceptable	Acceptable	Excellent
R^2	＜0.50	0.50-0.75	＞0.75
RPD	＜1.40	1.40-2.00	＞2.00

Results

The PNC of foxtail millet

To visually present the characteristics of the PNC data for foxtail millet under the experimental conditions, descriptive statistical analysis was conducted (*Table 2*). For the 120 samples obtained, they were randomly divided into calibration set (n = 90) and validation set (n = 30) in a 3:1 ratio. The maximum values for the PNC correction set and the validation set are 34.042 and 34.052, and the minimum values are 7.134 and 8.006, respectively. The overall distance is large, so there are significant differences in

http://www.aloki.hu ● ISSN 1589 1623 (Print) ● ISSN 1785 0037 (Online)
DOI: http://dx.doi.org/10.15666/aeer/2005_43914407

the data. The skewness is 0.485 and 0.457, respectively. The lower kurtosis and skewness also indicate that the dataset as a whole has an approximately normal distribution and can be further used for modeling and data analysis.

Table 2. *Descriptive statistical analysis for the PNC of foxtail millet*

Data type	Number	Min	Max	Mean	SD	Skewness	Kurtosis
Calibration set	90	7.134	34.042	19.059	8.730	0.485	-0.243
Validation set	30	8.006	34.052	19.488	8.701	0.457	-0.306

Analysis of changes in foxtail millet spectral reflectance

Due to interference from other external factors, the spectral data from 1350-1400 nm, 1800-1950 nm, and 2450-2500 nm were eliminated and not used. *Figure 1* reveals the spectral changes in the canopy of Jingu21 and Jingu28 at different growth stages and fertilization rates. With the T4 treatment as an example, the canopy spectra of the two cultivars were different in different growth stages, but the change trend was similar. Additionally, the spectral reflectance in the near-infrared region in the booting stage and the heading stage was higher than that in the other two growth stages. The change in the canopy structure led to a decrease in the spectral reflectance. In the filling stage, the spectral reflectance of the canopy was lower than that in the other three growth periods (*Fig. 1A, B*).

Figure 1C, D shows the raw spectrum changes of two foxtail millet cultivars at the heading stage under different fertilization rates. The reflectivity decreases in the visible region and increases in the near-infrared region. In the near-infrared region, the reflectivity is as high as 37%-62%, which is mainly due to the multiple reflection scattering of the inner structure of the leaf. With the increase in the nutrient level of the organic fertilizer, the nitrogen content, leaf area index and biomass of the plants increased, and the material accumulation and cell tissue contents increased correspondingly. In addition, the vegetation coverage, palisade tissue thickness, spongy tissue thickness and leaf thickness increased, resulting in an increase in the near-infrared reflectance. The figure also shows that the spectral reflectance of different organic fertilizer nutrient levels has a small difference in the visible range, while the difference gradually becomes larger in the near infrared band. In the near-infrared region, the spectral reflectance of the Jingu21 canopy showed a trend of first increasing and then decreasing. The spectral reflectance of the Jingu28 was T0 > T3 > T2 > T1 > T4.

Based on the spectral data of 120 samples, the spectral reflectance of the canopy spectral of Jingu21 and Jingu28 under different treatments was analyzed for variance. The results are shown in *Figure 2*, in the near-infrared region, Jingu21 and Jingu28 had some difference in spectral reflectance under 5 treatments. At 710-139 nm, 1532-1799 nm, and 1951-2431 nm, the spectral reflectance of Jingu21 differed by up to 5% between different treatments. At 545-1322 nm and 1439-1514 nm, the spectral reflectance of Jingu28 differed significantly between different treatments. It can be seen that there were spectral characteristic differences between foxtail millet under different treatments, and they can be distinguished.

Correlation analysis between the raw spectrum and the PNC

The correlation between the PNC and the spectral reflectance was analyzed and is shown in *Figure 3*. The visible light region (440-716 nm) was positively correlated with

http://www.aloki.hu ● ISSN 1589 1623 (Print) ● ISSN 1785 0037 (Online)
DOI: http://dx.doi.org/10.15666/aeer/2005_43914407

the PNC. The minimum absolute value of the correlation coefficient (R) was 0.249 near 539 nm, and the maximum absolute R value was 0.762 in the 670 nm band. The correlation between the PNC and the raw spectrum reflectance was negative at 717-1349 nm. The maximum absolute R value was 0.592 when the band was 933 nm, and the R value varied widely in the near-infrared region (1350-2158 nm).

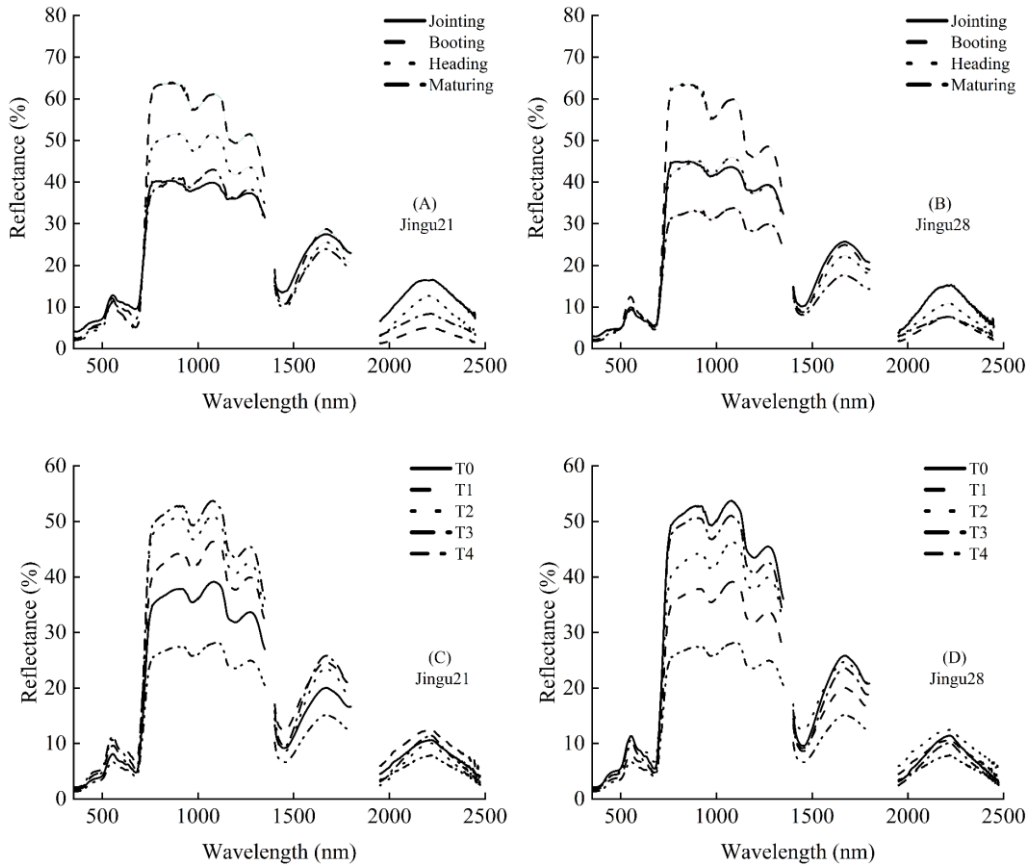

Figure 1. *Spectral curve changes of the two foxtail millet cultivars (Jingu21 and Jingu28). (A) and (B) represent the spectral curve changes at different growth and development stages. (C) and (D) represent the spectral curve changes of different organic fertilizer treatments*

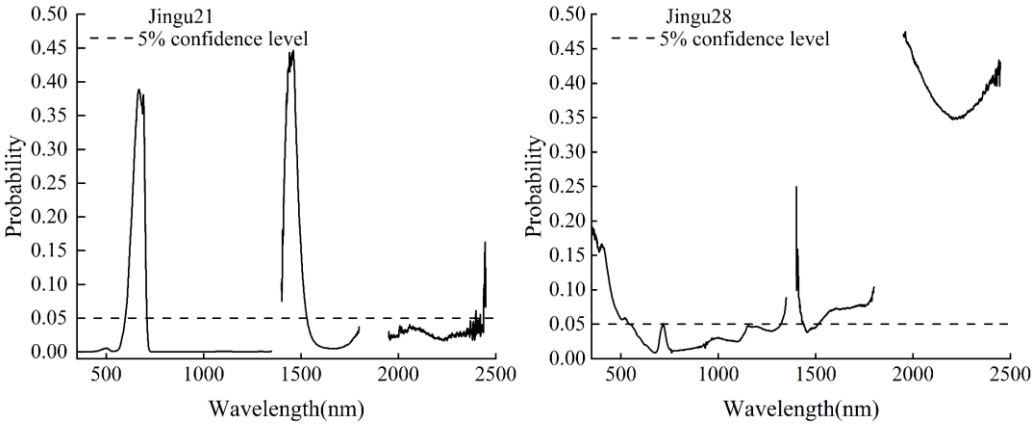

Figure 2. *Results of one-way ANOVA of foxtail millet canopy reflectance among the five treatments at different wavelength*

http://www.aloki.hu ● ISSN 1589 1623 (Print) ● ISSN 1785 0037 (Online)
DOI: http://dx.doi.org/10.15666/aeer/2005_43914407

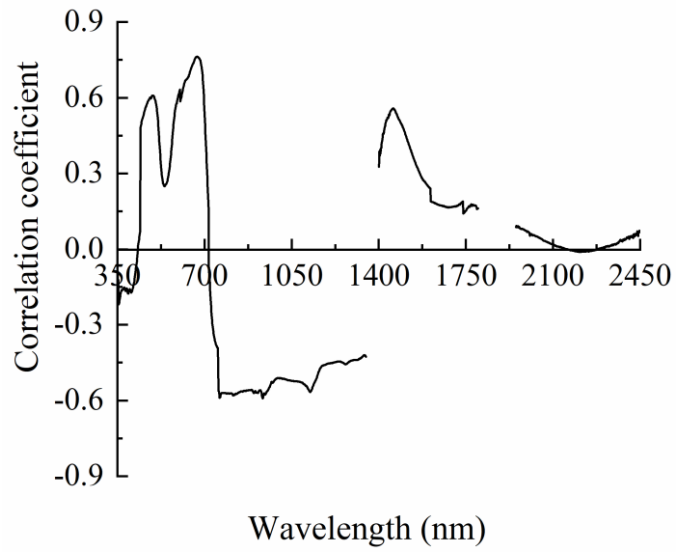

Figure 3. *Coefficient between the raw spectra and the PNC*

Correlation analysis of the wavelet coefficient and the PNC

The correlation between the wavelet coefficients obtained by db5, coif3, bior1.5, sym8, rbio3.1 and haar on the 2^1-2^{10} scale and the PNC was analyzed. The R value is expressed by the color depth in *Figure 4*. The correlation between the PNC and the wavelet coefficients is obviously positive and negative, and the difference in the R values among the different decomposition scales is obvious. Through the CWT, the detailed characteristic information related to the nitrogen content of foxtail millet was released layer by layer, and the wavelet coefficient information of each layer was different.

The maximum R value between the wavelet function and the PNC at different decomposition scales is shown in *Table 3*. bior1.5 showed the best correlation with the PNC, with an absolute value of 0.973 and a corresponding decomposition scale of 1. For coif3, db5, rbio3.1, sym8 and haar, the maximum absolute R values were 0.835, 0.834, 0.789, 0.784 and 0.770, respectively. The corresponding decomposition scales were 4, 4, 1, 4 and 2, respectively.

Table 3. *Comparison of the maximum R values between the wavelet coefficients and the PNC at different scales*

Decomposition scale	Maximum R					
	db5	**coif3**	**bior1.5**	**sym8**	**rbio3.1**	**haar**
2^1	-0.712	0.713	-0.973	-0.516	-0.789	-0.753
2^2	0.777	0.759	-0.809	0.628	-0.731	-0.77
2^3	0.793	0.804	-0.725	-0.721	-0.749	-0.729
2^4	0.834	-0.835	-0.737	-0.784	-0.724	-0.753
2^5	-0.827	0.805	-0.723	-0.722	-0.699	-0.717
2^6	0.698	0.709	-0.704	0.627	-0.655	-0.693
2^7	0.769	-0.626	-0.665	0.561	-0.538	-0.651
2^8	0.449	0.644	-0.505	-0.583	-0.432	-0.518
2^9	0.414	0.375	-0.431	0.353	-0.351	-0.425
2^{10}	-0.294	-0.293	-0.314	0.326	-0.191	-0.314

http://www.aloki.hu ● ISSN 1589 1623 (Print) ● ISSN 1785 0037 (Online)
DOI: http://dx.doi.org/10.15666/aeer/2005_43914407

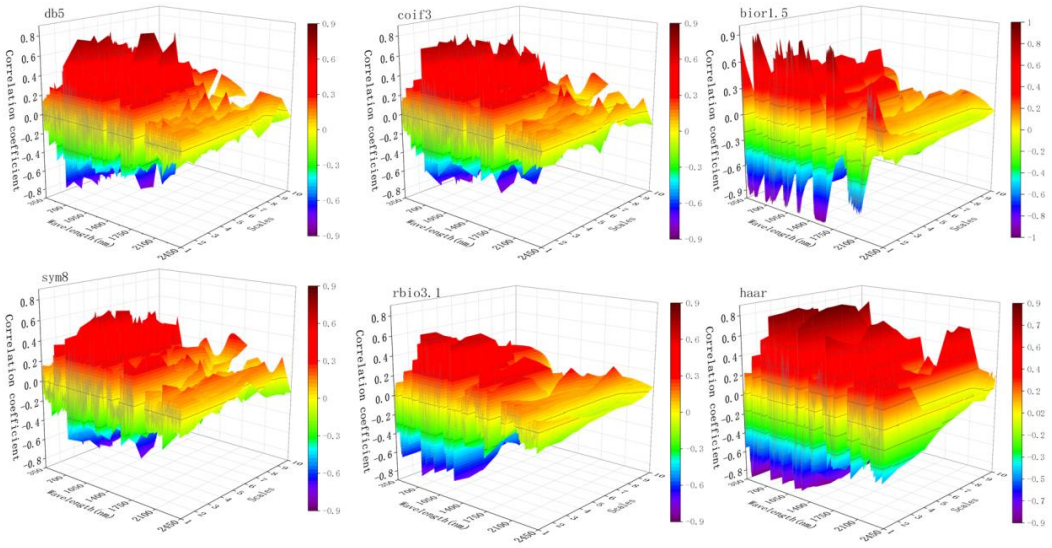

Figure 4. *Correlation analysis between the wavelet coefficients and the PNC based on six kinds of wavelet decomposition (n = 120)*

Establishment and verification of the PNC estimation model

The raw spectrum and CWT spectra were used as independent variables, and the PNC was used as a dependent variable; the PLSR, SVM and RF algorithms were used to characterize the relationship between the PNC and the spectral data. The results of the PNC model are shown in *Figure 5*. The results show that the predictive performances of the CWT spectra for the PNC compared to the raw spectrum and R^2, RMSE and RPD values were all significantly improved. However, significant differences were observed in the prediction accuracy of the different wavelet functions combined with the different machine learning algorithms. db5-RF, coif3-SVM, bior1.5-RF, sym8-RF, rbio3.1-SVM and haar-SVM had the best prediction performance. For the calibration dataset, the RPD values (RPD_{cal}) of the db5-RF, coif3-SVM, bior1.5-RF, sym8-RF, rbio3.1-SVM and haar-SVM models were 2.63, 2.34, 2.76, 2.14, 2.12 and 1.91, respectively, and these values were 168.36%, 60.27%, 181.63%, 118.37%, 45.21% and 30.82% higher than the corresponding values of the raw-spectrum model, respectively. For the validation dataset, the R^2 values (R^2_{val}) of the db5-RF, coif3-SVM, bior1.5-RF, sym8-RF, rbio3.1-SVM and haar-SVM models were 0.935, 0.890, 0.909, 0.874, 0.864 and 0.840, respectively, indicating that the estimation models have high degrees of fit and accuracy. Meanwhile, the RPD values of db5-RF, coif3-SVM, bior1.5-RF, sym8-RF, rbio3.1-SVM and haar-SVM were much greater than 2.0, indicating that these models have ideal predictive robustness and accuracy. Among them, the db5-RF model had the best prediction performance, with an RPD value of 3.32.

The measured and predicted values of the validated model were analyzed by the 1:1 line. As seen from the *Figure 6*, the sample points of both the measured and predicted values are basically distributed around the 1:1 line, and the model accuracy is high, indicating that these models can be used to estimate the PNC. The db5-RF model had the best prediction performance with an RPD value (RPD_{val}) of 3.32, indicating its ability to accurately estimate the PNC of foxtail millet. In summary, the SVM model with a 2^4-scale wavelet coefficient was obtained after db5 decomposition, and was the best model for establishing the canopy spectrum and nitrogen nutrition of foxtail millet.

http://www.aloki.hu ● ISSN 1589 1623 (Print) ● ISSN 1785 0037 (Online)
DOI: http://dx.doi.org/10.15666/aeer/2005_43914407

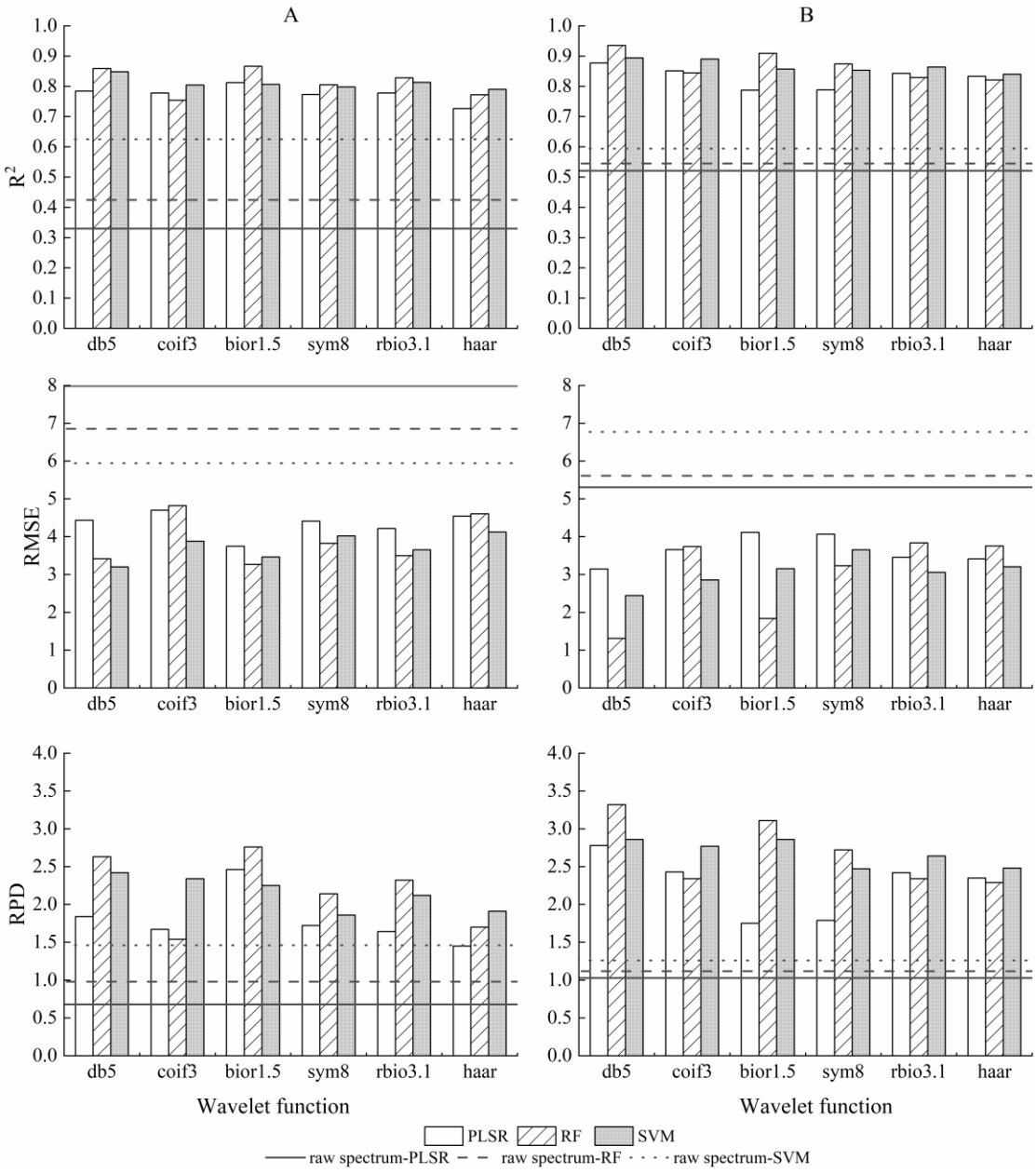

Figure 5. *The PNC model for foxtail millet (n = 120). A represents the calibration set, and B represents the validation set*

Discussion

Remote sensing-based crop phenotypic development provides a new way to monitor crop production and management, and the PNC can be remotely monitored to directly and quickly predict the photosynthetic performance and growth status of a plant using hyperspectral data (Jin et al., 2021; Weiss et al., 2020). In this study, the spectral reflectance of the foxtail millet canopy decreased gradually in the visible region and had a steep reflectance in the near-infrared region under different fertilization rates due to the application of the organic fertilizers, which affected the cellular structure of the vegetation leaves, removing the absorbing and scattering parts, and resulting in higher reflectivity values (Pinty et al., 2009). In the range of 740 to 1250 nm, the spectral

http://www.aloki.hu ● ISSN 1589 1623 (Print) ● ISSN 1785 0037 (Online)
DOI: http://dx.doi.org/10.15666/aeer/2005_43914407

reflectance of Jingu21 and Jingu28 performed differently under different treatments. The reason why the spectral reflectance of Jingu21 increased first and then decreased may be that with the increase of fertilizer, the phloem part of the leaves of foxtail millet decreased, and the utilization rate of photosynthetic products decreased (Cui et al., 2017). At the same time, the main stem of Jingu21 is 20-30 cm higher than that of Jingu28, and the fertilizer is too high, causing the foxtail millet to fall easily; Jingu28 has stronger tillering ability and need more nutrients, and its spectral reflectance increased with the increase of fertilizer amount. The stages of growth of a plant are associated with changes in cell structure, water content, biomass and function, which lead to changes in spectral reflectance during plant development (Bartlett et al., 2011; Li et al., 2014; Yu et al., 2014). Taking the T4 treatment as an example, the spectral reflectance first increased and then decreased with the progression of the growth stage and reached the maximum value at the booting stage. At this stage, the growth and development of foxtail millet are vigorous, photosynthesis is strengthened, and the ability of the plant to absorb nitrogen is enhanced, which affects the absorption and reflection of its canopy spectrum, thus leading to the strong absorption of visible light in this region. In addition, the reflectivity of the near-infrared region increases. In the near-infrared band, the water content of the plant increases its absorption and decreases its reflectivity (Im et al., 2008). This study showed that the spectral reflectance difference of foxtail millet under different treatments reached a significant level of 5%, which was consistent with Zhao et al. (2004). This may be due to the great influence of fertilization on various physiological and biochemical indices of foxtail millet, resulting in significant differences in the reflectance of the canopy spectral curve under different treatments (Serrano et al., 2000).

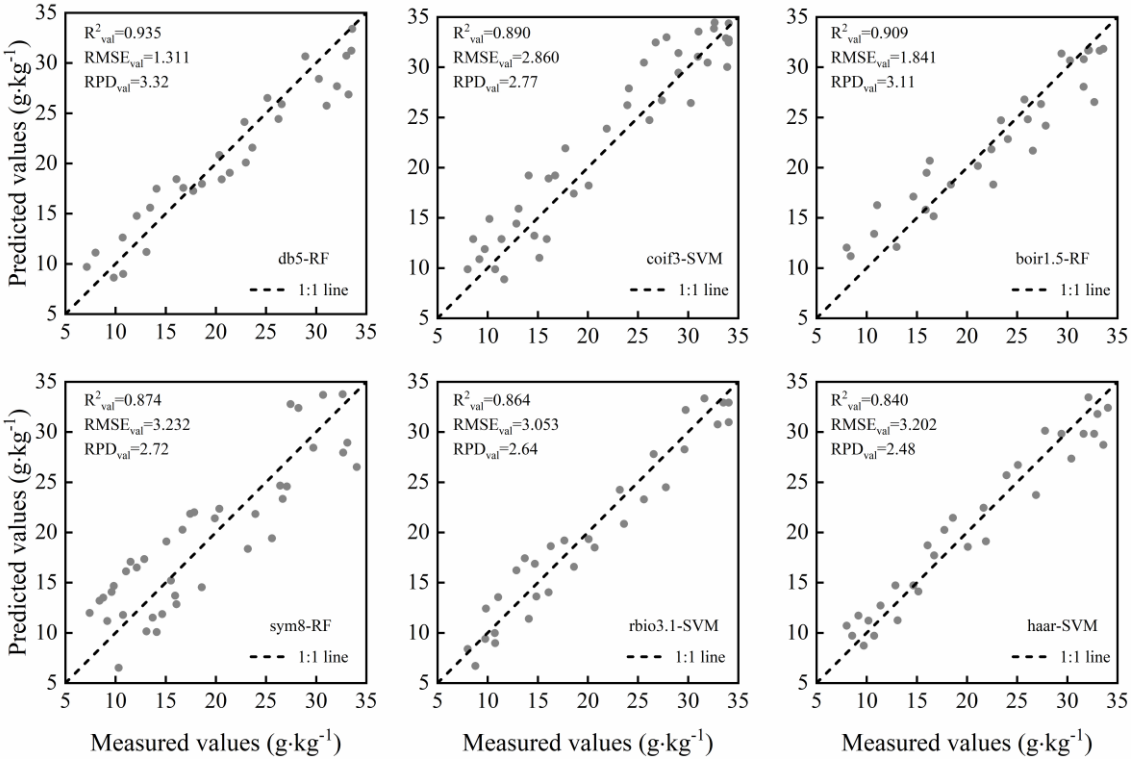

Figure 6. *Scatter plots of the measured and estimated PNCs of the validation set based on six kinds of wavelet functions (n = 30)*

http://www.aloki.hu ● ISSN 1589 1623 (Print) ● ISSN 1785 0037 (Online)
DOI: http://dx.doi.org/10.15666/aeer/2005_43914407

Many studies have shown that the PNC and the spectral reflectance have a good correlation (Guo et al., 2017; Boegh et al., 2021). In this study, we analyzed the correlation between the canopy spectra and the PNC and found that in the visible region, the nitrogen nutrition of foxtail millet was positively correlated with the spectral reflectance. However, in the near-infrared band region, the spectral reflectance was negatively correlated with nitrogen nutrition, which is consistent with the results of Alchanatis et al. (2005). The R value of the visible band was higher than that of the near-infrared band, which is mainly influenced by the canopy and the plant structure and does not reflect sensitivity to the PNC, while the visible band is sensitive to the PNC (Feng et al., 2008).

The wavelet coefficients obtained after the CWT decomposition showed a high correlation with the PNC because wavelet analysis can decompose hyperspectral data in space and frequency (Pinto et al., 2011; Zhang et al., 2020), and the physiological and biochemical composition of vegetation can be predicted by searching for optimal signals at different scales (He et al., 2018). Therefore, the CWT method can change the correlation of the PNC by decomposing the spectral data. The corresponding decomposition scales were found to appear before 2^8 when the R value between the six wavelet functions and the PNC was large. The results suggest that the CWT decomposition scale should be controlled at 2^8 in actual crop nitrogen monitoring. For each wavelet function, the maximum R value corresponds to a different decomposition scale.

The raw spectrum contains a large amount of information related to vegetation, but this information contains some redundancy (Fang et al., 2012), which makes the accuracy of the constructed models less than ideal. However, the CWT method can be used to further decompose the spectral data continuously, and the decomposed wavelet coefficients correspond to the raw spectrum. Thus, the fine signals in the spectral data can be extracted more effectively and the accuracy of the spectral monitoring model can be improved (Wang et al., 2020b). CWT spectral data can achieve a high accuracy in estimating chlorophyll, nitrogen, water, and photosynthetic rate data in vegetation, and such data are superior to the results of traditional methods (Liu et al., 2011; Koger et al., 2003; Yao et al., 2018). In this study, the CWT method was able to extract the weak spectral signal of foxtail millet well and achieve accurate estimation. These results are consistent with the results of previous studies (Li et al., 2018a, b). The different modeling results under different wavelet functions are shown in *Figure 5*, which is related to the nature of the wavelet functions. The performance of Daubechies (db5) in estimating the PNC of foxtail millet was the best. Therefore, the Daubechies family is recommended when estimating the PNC (Fu et al., 2020). However, this study was conducted under experimental conditions. Studies of each agronomic parameter and the different wavelet functions of foxtail millet for different regions, years, cultivars, and fertilization treatments are still needed to provide a theoretical basis to accurately estimate the growth of foxtail millet.

The SVM and RF algorithms, which have been successfully applied to estimate crop nitrogen levels can reveal the complicated nonlinear relationship between spectral characteristics and the crop nitrogen status (Marang et al., 2021). In this study, the SVM and RF models outperformed the PLSR model due to the presence of collinearity among the variables in the spectral data, which led to overfitting. Some overlapping spectral variables may contain invalid information for calibrating the model, such as noise and background, which can lead to inaccurate results. Therefore, a single approach for

http://www.aloki.hu ● ISSN 1589 1623 (Print) ● ISSN 1785 0037 (Online)
DOI: http://dx.doi.org/10.15666/aeer/2005_43914407

modeling the spectral data of vegetation is unfavorable, and optimized machine learning algorithms are increasingly used (Elsherbiny et al., 2021; Lu et al., 2020). However, spectral data contain many useless variables which can lead to complications in the models, and a relationship between the modeling approach and the data attributes may exist (Mehmood et al., 2012). The relationship between the variables and the modeling methods will be discussed in the future.

Conclusion

This study evaluated the performance of the PLSR, RF and SVM models of db5, coif3, bior1.5, sym8, rbio3.1 and haar in estimating PNC. Taking Jingu21 and Jingu28 as examples, the CWT method was performed on the raw spectrum at different decomposition scales to construct the PNC model. The results show that the model constructed by the CWT method is more accurate and reliable than the raw spectrum model. With the validation data, the R^2_{val} values of the db5-RF, coif3-SVM, bior1.5-RF, sym8-RF, rbio3.1-SVM and haar-SVM models were 0.935, 0.890, 0.909, 0.874, 0.864 and 0.840, respectively. The db5-RF model was found to perform the best (R^2_{val} = 0.935, $RMSE_{val}$ = 1.311, RPD_{val} = 3.32). The proposed method provides an intuitive way to monitor the nitrogen nutrient status of foxtail millet and thereby scientifically improve its quality and production.

Acknowledgements. This work was supported by the Research Program Sponsored by the State Key Laboratory of Sustainable Dryland Agriculture (in preparation), Shanxi Agricultural University (No. 202003-6), and the Key Research and Development Program of Shanxi Province, China (201903D211002-01, 201703D211001).

REFERENCES

[1] Alchanatis, V., Schmilovitch, Z., Meron, M. (2005): In-field assessment of single leaf nitrogen status by spectral reflectance measurements. – Precision Agriculture 6(1): 25-39.
[2] Ampe, E. M., Hestir, E. L., Bresciani, M., Salvadore, E. (2013): A wavelet approach for estimating chlorophyll a form inland waters with reflectance spectroscopy. – IEEE Geoscience and Remote Sensing Letters 11(1): 89-33.
[3] Bartlett, M. K., Ollinger, S. V., Hollinger, D. Y., Wicklein, H. F., Richardson, A. D. (2011): Canopy-scale relationships between foliar nitrogen and albedo are not observed in leaf reflectance and transmittance within temperate deciduous tree species. – Botany 89: 491-497.
[4] Bechlin, M. A., Fortunato, F. M., Silva, R. M. D., Ferreira, E. C., Neto, J. A. G. (2014): A simple and fast method for assessment of the nitrogen–phosphorus–potassium rating of fertilizers using high-resolution continuum source atomic and molecular absorption spectrometry. – Spectrochimica Acta Part B: Atomic Spectroscopy 101: 240-244.
[5] Blackburn, G., Ferwerda, J. (2008): Retrieval of chlorophyll concentration from leaf reflectance spectra using wavelet analysis. – Remote Sensing of Environment 112(4): 1614-1632.
[6] Bleiholder, H., Buhr, L., Eicke, H., Feller, C., Hack, H., Hess, M., Klose, R., Lancashire, P. D., MEIER, U., Stauss, R., Weber, E., von den Boom, T. (2001): Growth stages of mono- and dicotyledonous plants. – BBCH Monograph 158.
[7] Boegh, E., Soegaard, H., Broge, N., Hasager, C. B., Jensen, N. O., Schelde, K., Thomsen, A. (2021): Airborne multi-spectral data for quantifying leaf area index, nitrogen con-

http://www.aloki.hu ● ISSN 1589 1623 (Print) ● ISSN 1785 0037 (Online)
DOI: http://dx.doi.org/10.15666/aeer/2005_43914407

centration, and photosynthetic efficiency in agriculture. – Remote Sensing of Environment 81(2-3): 179-193.

[8] Chen, S., Hu, T., Luo, L., He, Q., Li, H. (2020): Rapid estimation of leaf nitrogen content in apple-trees based on canopy hyperspectral reflectance using multivariate methods. – Infrared Physics and Technology 111: 103542.

[9] Chen, D. S., Zhang, F., Tan, M. L., Chan, N. W., Shi, J. C., Liu, C. J., Wang, W. W. (2022): Improved Na^+ estimation from hyperspectral data of saline vegetation by machine learning. – Computers and Electronics in Agriculture 196: 106862.

[10] Cheng, T., Rivard, B., Sánchez-Azofeifa, G. A., Feng, J., Calvo-Polanco, M. (2010): Continuous wavelet analysis for the detection of green attack damage due to mountain pine beetle infestation. – Remote Sensing of Environment 114(4): 899-910.

[11] Cheng, T., RiañO, D., Ustin, S. L. (2014): Detecting diurnal and seasonal variation in canopy water content of nut tree orchards from airborne imaging spectroscopy data using continuous wavelet analysis. – Remote Sensing of Environment 143: 39-53.

[12] Clevers, J. G., Kooistra, L., Marnix, V. D. B. (2017): Using Sentinel-2 data for retrieving LAI and leaf and canopy chlorophyll content of a potato crop. – Remote Sensing 9(5): 405.

[13] Cui, J. H., Zhao, J., Meng, J., Liu, M., Zhao, Y., Song, S. J., Xia, X. Y., Li, S. G. (2017): Effect of ammonium nitrogen and nitrate nitrogen on the morphology and biomass of foxtail millet (*Setaria italic* L.). – Journal of Agricultural Science and Technology 19(10): 66-72.

[14] Datt, B. (1999): Visible/near infrared reflectance and chlorophyll content in Eucalyptus leaves. – International Journal of Remote Sensing 20(14): 2741-2759.

[15] Dong, S. K., Gong, Z. P., Wei, Z. U. (2010): Effects of nitrogen nutrition levels on N-accumulation and yields of soybean. – Plant Nutrition and Fertilizer Science 16: 65-70.

[16] Eitel, J. U. H., Magney, T. S., Vierling, L. A., Brown, T. T., Huggins, D. R. (2014): LiDAR based biomass and crop nitrogen estimates for rapid, non-destructive assessment of wheat nitrogen status. – Field Crops Research 159: 21-32.

[17] Elsherbiny, O., Fan, Y., Zhou, L., Qiu, Z. (2021): Fusion of feature selection methods and regression algorithms for predicting the canopy water content of rice based on hyperspectral data. – Agriculture 11(1): 51.

[18] Fang, Q., Tian, H. (2012): A review of hyperspectral remote sensing in vegetation monitoring. – Remote Sensing Technology and Application 13(1): 62-69.

[19] Feng, W., Yao, X., Zhu, Y., Tian, Y. C., Cao, W. X. (2008): Monitoring leaf nitrogen status with hyperspectral reflectance in wheat. – European Journal of Agronomy 28(3): 394-404.

[20] Feng, W., Zhang, H. Y., Zhang, Y. S., Qi, S. L., Guo, T. C. (2016): Remote detection of canopy leaf nitrogen concentration in winter wheat by using water resistance vegetation indices from in-situ hyperspectral data. – Field Crops Research 198: 238-246.

[21] Fu, Y., Yang, G., Li, Z., Li, H., Li, Z., Xu, X., Chen, L. (2020): Progress of hyperspectral data processing and modelling for cereal crop nitrogen monitoring. – Computers and Electronics in Agriculture 172: 105321.

[22] Guo, B. B., Qi, S. L., Heng, Y. R., Duan, J. Z., Zhang, H. Y., Wu, Y. P., Zhu, Y. J. (2017): Remotely assessing leaf N uptake in winter wheat based on canopy hyperspectral red-edge absorption. – European Journal of Agronomy 82: 113-124.

[23] He, L., Song, X., Feng, W., Guo, B. B., Zhang, Y. S., Wang, Y. H., Wang, C. Y., Guo, T. C. (2016): Improved remote sensing of leaf nitrogen concentration in winter wheat using multi-angular hyperspectral data. – Remote Sensing of Environment 174: 122-133.

[24] He, R. Y., Li, H., Qiao, X. J., Jing, J. B. (2018): Using wavelet analysis of hyperspectral remote-sensing data to estimate canopy chlorophyll content of winter wheat under stripe rust stress. – International Journal of Remote Sensing 39: 4059-4076.

http://www.aloki.hu ● ISSN 1589 1623 (Print) ● ISSN 1785 0037 (Online)
DOI: http://dx.doi.org/10.15666/aeer/2005_43914407

[25] Hong, S., Liu, N., Li, W., Chen, L., Yang, L., Li, M., Zhang, Q. (2018): Water content detection of potato leaves based on hyperspectral image. – IFAC-PapersOnLine 51(17): 443-448.
[26] Im, J., Jensen, J. R. (2008): Hyperspectral remote sensing of vegetation. – Geography Compass 2(6): 1943-1961.
[27] Jia, G. Q., Huang, X. H., Zhi, H., Zhao, Y., Zhao, Q., Li, W. J., Chai, Y., Yang, L. F., Liu, K. Y., Lu, H. Y., Zhu, C. R., Lu, Y. Q., Zhou, C. C., Fan, D. L., Weng, Q. J., Guo, Y. L., Huang, T., Zhang, L., Lu, T. T., Feng, Q., Hao, H. F., Liu, H. K., Li, P., Zhang, N., Li, Y. H., Guo, E. H., Wang, S. J., Wang, S. Y., Liu, J. R., Zhang, W. F., Chen, G. Q., Zhang, B. J., Li, W., Wang, Y. F., Li, H. Q., Zhao, B. H., Li, J. Y., Diao, X. M., Han, B. (2013): A haplotype map of genomic variations and genome-wide association studies of agronomic traits in foxtail millet (*Setaria italica*). – Nature Genetics 45: 957-961.
[28] Jin, X., Zarco-Tejada, P. J., Schmidhalter, U., Reynolds, M. P., Hawkesford, M. J., Varshney, R. K., Yang, T., Nie, C., Li, Z., Ming, B. O., Xiao, Y., Xie, Y., Li, S. (2021): High-throughput estimation of crop traits: A review of ground and aerial phenotyping platforms. – IEEE Geoscience and Remote Sensing Magazine 9(1): 200-231.
[29] Koger, C. H., Bruce, L. M., Shaw, D. R., Reddy, K. N. (2003): Wavelet analysis of hyperspectral reflectance data for detecting pitted morning glory (Ipomoea lacunose) in soybean (Glycine max). – Remote Sensing of Environment 86: 108-119.
[30] Li, F., Mistele, B., Hu, Y., Chen, X., Schmidhalter, U. (2014): Optimising three-band spectral indices to assess aerial N concentration, N uptake and aboveground biomass of winter wheat remotely in China and Germany. – ISPRS Journal of Photogrammetry and Remote Sensing 92: 112-123.
[31] Li, D., Wang, C., Liu, W., Peng, Z., Huang, S., Huang, J., Chen, S. (2016): Estimation of litchi (*Litchi chinensis* Sonn) leaf nitrogen content at different growth stages using canopy reflectance spectra. – European Journal of Agronomy 80: 182-194.
[32] Li, D., Wang, X., Zheng, H., Zhou, K., Yao, X., Tian, Y., Cheng, T. (2018b): Estimation of area and mass based leaf nitrogen contents of wheat and rice crops from water-removed spectra using continuous wavelet analysis. – Plant Methods 14(1): 1-20.
[33] Li, D., Cheng, T., Jia, M., Zhou, K., Lu, N., Yao, X., Cao, W. (2018a): PROCWT: Coupling PROSPECT with continuous wavelet transform to improve the retrieval of foliar chemistry from leaf bidirectional reflectance spectra. – Remote Sensing of Environment 206: 1-14.
[34] Li, Z., Jin, X., Yang, G., Drummond, J., Yang, H., Clark, B., Zhao, C. (2018c): Remote sensing of leaf and canopy nitrogen status in winter wheat (*Triticum aestivum* L.) based on N-PROSAIL model. – Remote Sensing 10(9): 1-18.
[35] Lin, D., Li, G., Zhu, Y., Liu, H., Jiao, Q. (2021): Predicting copper content in chicory leaves using hyperspectral data with continuous wavelet transforms and partial least squares. – Computers and Electronics in Agriculture 187: 106293.
[36] Liu, M., Liu, X., Ding, W., Wu, L. (2011): Monitoring stress levels on rice with heavy metal pollution from hyperspectral reflectance data using wavelet-fractal analysis. – International Journal of Applied Earth Observation and Geoinformation 13(2): 246-255.
[37] Lu, H. Y., Zhang, J. P., Liu, K. B., Wu, N. Q., Li, Y. M., Zhou, K. S., Ye, M. L., Zhang, T. Y., Zhang, H. J., Yang, X. Y., Shen, L. C., Xu, D. K., Li, Q. (2009): Earliest domestication of common millet (Panicum miliaceum) in East Asia extended to 10,000 years ago. – Proceedings of the National Academy of Sciences 106(18): 7367-7372.
[38] Lu, X., Zhang, S., Tian, Y., Li, Y., Wen, R., Tsou, J., Zhang, Y. (2020): Monitoring Suaeda salsa spectral response to salt conditions in coastal wetlands: A case study in dafeng elk national nature reserve, China. – Remote Sensing 12(17): 2700.
[39] Mahajan, P., Bera, M. B., Panesar, P. S., Chauhan, A. (2021): Millet starch: a review. – International Journal of Biological Macromolecules 180(3): 61-79.

http://www.aloki.hu ● ISSN 1589 1623 (Print) ● ISSN 1785 0037 (Online)
DOI: http://dx.doi.org/10.15666/aeer/2005_43914407

[40] Mao, H., Gao, H., Zhang, X., Kumi, F. (2015): Nondestructive measurement of total nitrogen in lettuce by integrating spectroscopy and computer vision. – Scientia Horticulturae 184: 1-7.
[41] Marang, I. J., Filippi, P., Weaver, T. B., Evans, B. J., Whelan, B. M., Bishop, T. F., Roth, G. (2021): Machine learning optimised hyperspectral remote sensing retrieves cotton nitrogen status. – Remote Sensing 13(8): 1428.
[42] Mehmood, T., Liland, K. H., Snipen, L., Sæbø, S. (2012): A review of variable selection methods in partial least squares regression. – Chemometrics and Intelligent Laboratory Systems 118: 62-69.
[43] Pinto, L. A., Galv˜ao, R. K. H., Araújo, M. C. U. (2011): Influence of wavelet transform settings on NIR and MIR spectrometric analyses of diesel, gasoline, corn and wheat. – Journal of the Brazilian Chemical Society 22(1): 179-186.
[44] Pinty, B., Lavergne, T., Widlowski, J. L., Gobron, N., Verstraete, M. (2009): On the need to observe vegetation canopies in the near-infrared to estimate visible light absorption. – Remote Sensing of Environment 113(1): 10-23.
[45] Ranjan, R., Chopra, U. K., Sahoo, R. N., Singh, A. K., Pradhan, S. (2012): Assessment of plant nitrogen stress in wheat (*Triticum aestivum* L.) through hyperspectral indices. – International Journal of Remote Sensing 33(20): 6342-6360.
[46] Rivard, B., Feng, J., Gallie, A., Sanchez-Azofeifa, A. (2008): Continuous wavelets for the improved use of spectral libraries and hyperspectral data. – Remote Sensing of Environment 112(6): 2850-2862.
[47] Rivera-Caicedo, J. P., Verrelst, J., Muñoz-Marí, J., Camps-Valls, G., Moreno, J. (2017): Hyperspectral dimensionality reduction for biophysical variable statistical retrieval. – ISPRS Journal of Photogrammetry and Remote Sensing 132: 88-101.
[48] Serrano, L., Filella, L., Penuelas, J. (2000): Remote sensing of biomass and yield of winter wheat under different nitrogen supplies. – Crop Science 40: 723 − 731.
[49] Stroppiana, D., Boschetti, M., Brivio, P. A., Bocchi, S. (2009): Plant nitrogen concentration in paddy rice from field canopy hyperspectral radiometry. – Field Crop Research 111(1-2): 119-129.
[50] Tan, K., Wang, S., Song, Y., Liu, Y., Gong, Z. (2017): Estimating nitrogen status of rice canopy using hyperspectral reflectance combined with BPSO-SVR in cold region. – Chemometrics and Intelligent Laboratory Systems 172: 68-79.
[51] Tao, C., Rivard, B., Sánchez-Azofeifa, A. G., Féret, J. B., Jacquemoud, S., Ustin, S. L. (2012): Predicting leaf gravimetric water content from foliar reflectance across a range of plant species using continuous wavelet analysis. – Journal of Plant Physiology 169(12): 1134-1142.
[52] Tarpley, L., Reddy, K. R., Sassenrath-Cole, G. F. (2000): Reflectance indices with precision and accuracy in predicting cotton leaf nitrogen concentration. – Crop Science 40(6): 1814-1819.
[53] Thorp, K. R., Wang, G., Bronson, K. F., Badaruddin, M., Mon, J. (2017): Hyperspectral data mining to identify relevant canopy spectral features for estimating durum wheat growth, nitrogen status, and grain yield. – Computers and Electronics in Agriculture 136: 1-12.
[54] Tian, Y. C., Gu, K. J., Chu, X., Yao, X., Cao, W. X., Zhu, Y. (2014): Comparison of different hyperspectral vegetation indices for canopy leaf nitrogen concentration estimation in rice. – Plant and Soil 376(1-2): 193-209.
[55] Virmani, J., Kumar, V., Kalra, N., Khandelwal, N. (2013): SVM-based characterization of liver ultrasound images using wavelet packet texture descriptors. – Journal of Digital Imaging 26(3): 530-543.
[56] Viscarra, R. A., Mcglynn, R. N., Mcbratney, A. B. (2007): Determining the composition of mineral-organic mixes using UV-VIS-NIR diffuse reflectance spectroscopy. – Geoderma 137(1/2): 70-82.

http://www.aloki.hu ● ISSN 1589 1623 (Print) ● ISSN 1785 0037 (Online)
DOI: http://dx.doi.org/10.15666/aeer/2005_43914407

[57] Wang, H. F., Huo, Z. G., Zhou, G. S., Liao, Q. H., Feng, H. K., Wu, L. (2016): Estimating leaf SPAD values of freeze-damaged winter wheat using continuous wavelet analysis. – Plant Physiology and Biochemistry Ppb 98: 39-45.
[58] Wang, G. D., Wang, Q. X., Su, Z. L., Zhang, J. H. (2020a): Predicting copper contamination in wheat canopy during the full growth period using hyperspectral data. – Environmental Science and Pollution Research 27(31): 39029-39040.
[59] Wang, Z., Chen, J., Fan, Y., Cheng, Y., Wu, X., Zhang, J., Yang, F. (2020b): Evaluating photosynthetic pigment contents of maize using UVE-PLS based on continuous wavelet transform. – Computers and Electronics in Agriculture 169: 105160.
[60] Weiss, M., Jacob, F., Duveiller, G. (2020): Remote sensing for agricultural applications: A meta-review. –Remote Sensing of Environment 236: 111402.
[61] Yao, X., Si, H. Y., Cheng, T., Jia, M., Chen, Q., Tian, Y. C., Zhu, Y., Cao, W. X., Chen, C. Y., Cai, J. Y., Gao, R. R. (2018): Hyperspectral estimation of canopy leaf biomass phenotype per ground area using a continuous wavelet analysis in wheat. – Frontiers in Plant Science 9: 1360.
[62] Yu, K., Lenz-Wiedemann, V., Chen, X., Bareth, G. (2014): Estimating leaf chlorophyll of barley at different growth stages using spectral indices to reduce soil background and canopy structure effects. – ISPRS Journal of Photogrammetry and Remote Sensing 97: 58-77.
[63] Zadoks, J. C., Chang, T. T., Konzak, C. F. (1974): A decimal code for the growth stages of cereals. – Weed Research 14(6): 415-421.
[64] Zhang, J., Yuan, L., Pu, R., Loraamm, R. W., Yang, G., Wang, J. (2014): Comparison between wavelet spectral features and conventional spectral features in detecting yellow rust for winter wheat. – Computers and Electronics in Agriculture 100: 79-87.
[65] Zhang, J. Y., Sun, H., Gao, D. H., Qiao, L., Liu, N., Li, M. Z., Zhang, Y. (2020): Detection of canopy chlorophyll content of corn based on continuous wavelet transform analysis. – Remote Sensing 12(17): 2741.
[66] Zhao, D. H., Li, J. L., Song, Z. J., Qi, J. G. (2004): Difference of canopy spectral reflectance to nitrogen nutrient in cotton with different nitrogen applications. – Acta Agronomica Sinica 30(11): 1169-1172.
[67] Zhou, K., Cheng, T., Zhu, Y., Cao, W., Ustin, S. L., Zheng, H., Tian, Y. (2018): Assessing the impact of spatial resolution on the estimation of leaf nitrogen concentration over the full season of paddy rice using near-surface imaging spectroscopy data. – Frontiers in Plant Science 9: 964.

http://www.aloki.hu ● ISSN 1589 1623 (Print) ● ISSN 1785 0037 (Online)
DOI: http://dx.doi.org/10.15666/aeer/2005_43914407